Performance of Five-Axis Machine Tool and Intelligent Machining Process

Tzu-Chi Chan (tcchan@nfu.edu.tw)
National Formosa University
Hsin-Hsien Lin
National Formosa University

Research Article

Keywords: Five-axis machine tool, Finite element method, Static stiffness, Modal analysis, Modal test, Abductory Induction Mechanism

Posted Date: September 21st, 2021

DOI: https://doi.org/10.21203/rs.3.rs-911681/v1

Performance of five-axis machine tool and intelligent machining process

Tzu-Chi Chan*, Hsin-Hsien Lin

Department of Mechanical and Computer-Aided Engineering,
National Formosa University, Yunlin, Taiwan

*Corresponding author: **Tzu-Chi Chan**, tcchan@nfu.edu.tw

A B S T R A C T

In this study, the processing performance of a five-axis machine tool was analyzed to identify processing weaknesses as the basis for subsequent structural improvements. Data were then integrated through the Abductory Induction Mechanism (AIM) polynomial neural network to predict intelligent processing quality, and an in-depth investigation was conducted by importing processing parameters to predict the surface quality of the finished product.

The finite element analysis method was used to analyze the static and dynamic characteristics of the whole machine and to test the structural modal frequency and vibration shape. For modal testing, the experiment used various equipment, including impact hammers, accelerometers, and signal extractors. Subsequent planning of modal frequency band processing experiments was conducted to verify the influence of natural frequencies on the processing level. Finally, according to the machine processing characteristics, a processing experiment was planned. The measurement record was used as the training data of the AIM polynomial neural network to establish the processing quality prediction model.

After analysis and an actual machine test comparison, the three-axis static rigidity values of the machine were X: 1.63 Kg/μm, Y: 1.93 Kg/μm, and Z: 3.95 Kg/μm. The modal vibration shape maximum error of the machine was within 6.2%. The processing quality prediction model established by the AIM polynomial neural network could input processing parameters to

achieve the surface roughness prediction value, and the actual relative error of the Ra value was within 0.1 μm.

Based on the results of cutting experiments, the influence of the dynamic characteristics of the machine on the processing quality was obtained, especially in the modal vibration environment, which had an adverse effect on the surface roughness. Hence, the surface roughness of the workpiece processed by the machine could be predicted.

Keywords: Five-axis machine tool, Finite element method, Static stiffness, Modal analysis, Modal test, Abductory Induction Mechanism

Nomenclature

CPM：Complexity penalty factor

FSE ：Square error

KP ：Complexity penalty

PSE ：Predicted squared error

1 Introduction

A machine tool must have sufficient rigidity and optimized design considerations in the structural analysis stage to facilitate the best performance of the machine and to develop intelligent processing functions based on excellent machine performance. Therefore, many studies have been conducted in this area. Eynian [1] used mathematical models to determine the processing parameters that are required for stable, high-performance, and high-speed processing. These mathematical models must accurately measure the modal parameters of the processing system. Tang et al. [2] proposed a nonlinear tool mark coefficient recognition

method using finite amplitude. The results showed that the size distribution of the critical depth of the cut is affected by the process damping, and the percentage increase in the cut depth is closely related to the tool direction and the frequency response function (FRF). Liu et al. [3] considered the effect of elastic interaction to analyze the influence of the anchor bolt pre-tightening sequence on the pre-tightening state. The results showed that the pre-tightening sequence from the middle to the side can ensure uniform deformation of the machine bed.

Muñoz-Escalona et al. [4] studied a geometric model for predicting the surface roughness of square inserts in face milling. The Taguchi method was used as an experimental design, and the surface roughness of the milled surface was measured using a non-contact profiler. Zhao et al. [5] proposed a surface-roughness prediction model and showed that the tool posture has a significant influence on the surface roughness, which means that the angle of the tool can be controlled to improve the surface roughness of the processing. Wang et al. [6] proposed a five-axis tooth surface milling surface roughness control method using feed rate optimization based on surface topography analysis. According to this model, the influence of tool runout and workpiece curvature on the surface profile was analyzed.

Wang et al. [7] proposed a model by which the predicted surface morphology was determined, and the factors affecting the development trend of roughness were analyzed. Tomov et al. [8] suggested the relationship between the parameter prediction model and thesurface roughness formation process. Das et al. [9] explored artificial neural networks and predicted the cutting force and surface roughness generated during CNC milling. García-Plaza et al. [10] optimized surface roughness monitoring by focusing on vibration signal analysis. Accordingly, the signal statistical measurements and frequency bands were correlated with surface roughness. Rasagopal et al. [11] studied the influence of processing parameters on the surface roughness and cutting force of mixed aluminum metal matrix composites. The results were optimized and analyzed using the Taguchi method. Mansour et al. [12] developed a

mathematical model of surface roughness based on the cutting speed, feed rate, and cutting axial depth. Abouelatta [13] identified a correlation between surface roughness and cutting vibration during turning, and they derived a mathematical model of the predicted roughness parameters based on cutting parameters and machine tool vibration. Lin et al. [14] constructed a prediction model for surface roughness and cutting force. Once the machining parameters are given, the surface roughness and cutting force can be predicted through the network. Ostasevicius et al. [15] proposed a method to improve the surface roughness. The method is based on the excitation of a specific higher vibration mode of the turning tool and it reduces the harmful vibration in the machine tool and workpiece system by increasing the energy dissipation inside the tool material. Sahin et al. [16] found that the feed rate is the main factor affecting the surface roughness, and good agreement between the predicted and experimental surface roughness was observed within a reasonable range. Öktem et al. [17] studied the best cutting conditions to achieve the smallest surface roughness in mold surface milling. Lalwani et al. [18] studied the influence of cutting parameters on the cutting force and surface roughness in finishing hard turning. PauloDavim et al. [19] established a surface roughness prediction model using neural networks using cutting conditions, such as cutting speed, feed rate, and cutting depth, as influencing factors. Their analysis showed that the cutting speed and feed rate have a significant effect on reducing the surface roughness, while the depth of cut has the smallest effect. Liu et al. [20] proposed a model that can provide valuable information about the effects of cutting parameters on surface roughness. Diniz et al. [21] studied the effect of changing the cutting speed, feed, and nose radius on the surface roughness of a workpiece with and without cutting fluid. Muthukrishnan et al. [22] used the input parameters of the cutting depth, cutting speed, and feed, and the output parameter was the surface finish of the machined part. The surface finish of machining can be predicted under cutting conditions within the operating range. Rawangwong et al. [23] used tungsten carbide tools for the face milling of

semi-solid metal AA7075. They used Taguchi's experimental method to determine the three control factors— the cutting speed, feed rate, and depth of cut—to obtain more satisfactory surface roughness. Wang et al. [24] used an abductive network to construct a network model, and one output was surface roughness. Chen et al. [25] proposed an AIM polynomial network with the material properties provided as input to generate a model that predicts the tool geometry.

The machine tool industry is gradually advancing in terms of intelligent machine tool manufacturing. Accordingly, this study recorded the measurement results of the cutting experiment under different dynamic characteristics and parameters of the machine in the cases of the respective processing parameters, construction methods, and cutting materials. It employed a similar neural network construction to be effective. It is expected that the model for predicting the surface quality of the finished product can reduce processing costs and can thus be used as a basis for follow-up control experiments. When the processing parameters are imported, the surface roughness can be predicted using the network.

2 Materials and Methods

The experimental hardware equipment used in this research included a five-axis machine tool, LM load cell, German Mahr sensor probe, Millimar C1200 displacement display meter (LVDT), impact hammer (Kistler 9726A20000), accelerometer (Endevco Model 65-100), spectrum analyzer, SE-4000 non-contact surface roughness meter, and Olympus STM 6 high-precision tool microscope. The software included the finite element analysis software ANSYS Workbench, spectrum analysis software Novian, modal post-processing software MEscope, Static Stiffness acquisition and analysis software, and the AIM polynomial neural network. The experimental process is illustrated in Fig. 1.

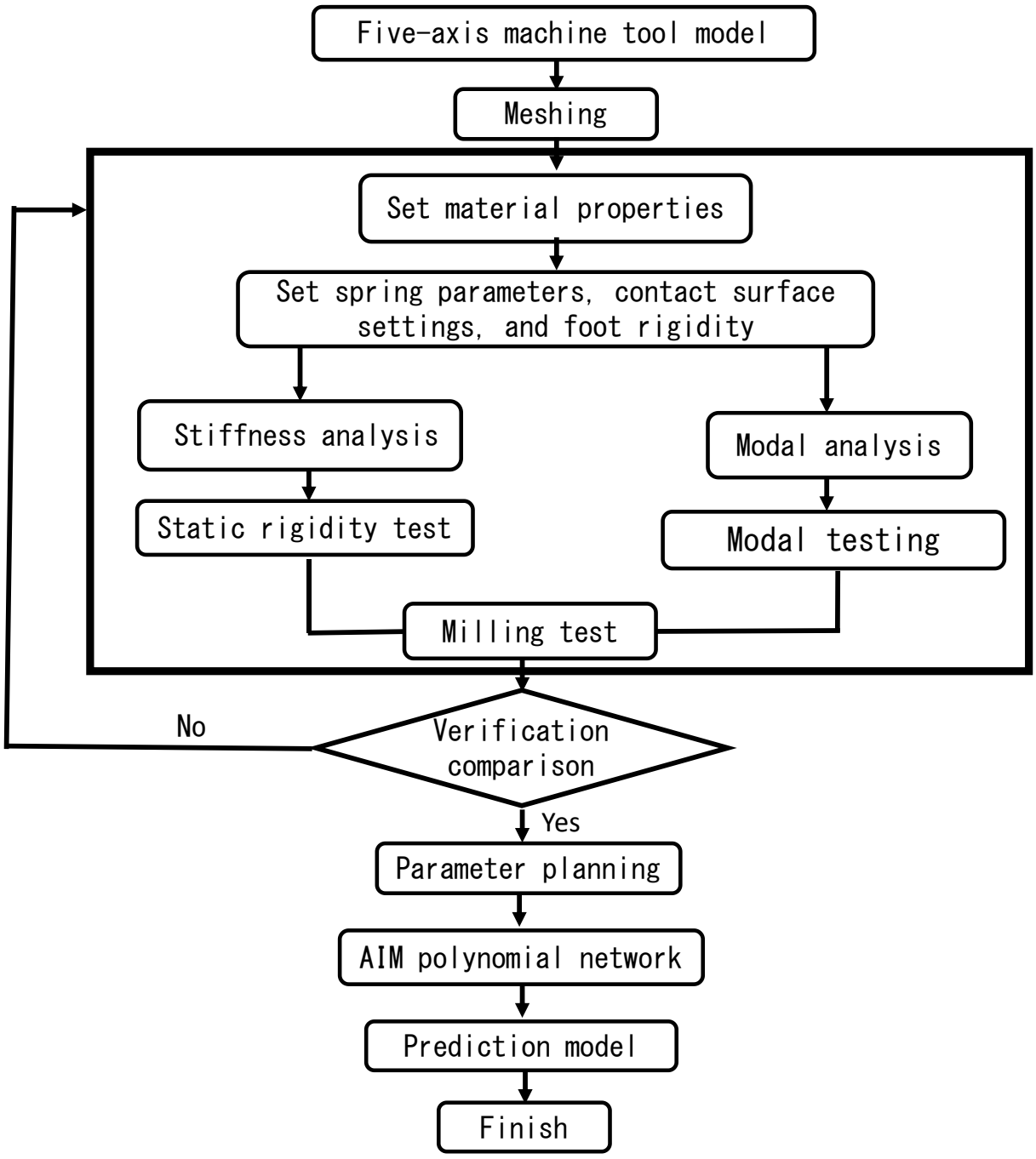

Fig. 1 Research flow chart

3 Analysis and Test

When the machine is processing, the relative movement of the spindle end to the work platform will affect the surface quality and accuracy of the workpiece. Therefore, static rigidity simulation analysis was conducted for the spindle relative to the work platform. According to the analysis results, the X-axis relative displacement was 182.7 μm, and the static rigidity value was 1.64 (Kg/μm). The Y-axis relative displacement was 145.5 μm, and the static rigidity value

was 2.06 (Kg/μm).

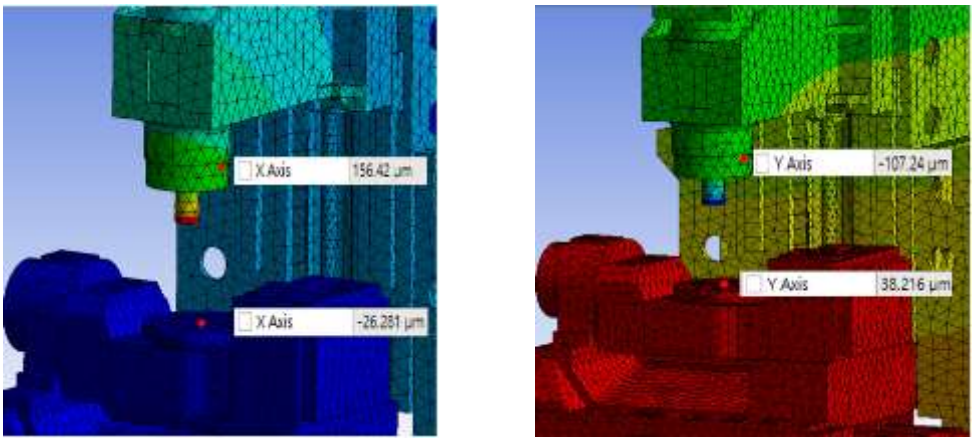

(a) Static rigidity analysis-X axis (b) Static rigidity analysis-Y axis

Fig. 2 Spindle vs. rotating worktable: analysis of static rigidity in X and Y axes

In the static rigidity experiment, the force application point was 100 mm below the nose of the spindle. The rotary table was used as a benchmark to test the corresponding axial rigidity of the machine spindle, as shown in Fig. 3. According to the experimental results, the static rigidity values of the spindle end corresponding to the X and Y axes measured on the basis of the rotating table were 1.63 (Kg/μm) and 1.93 (Kg/μm), respectively.

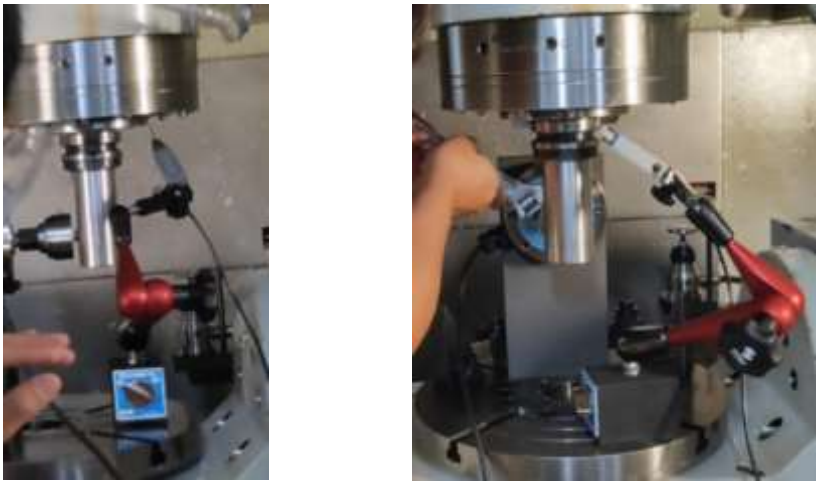

(a) X-axis static rigidity test (b) X-axis static rigidity test

Fig. 3 Entire machine processing platform corresponding to the static rigidity of X and Y axes

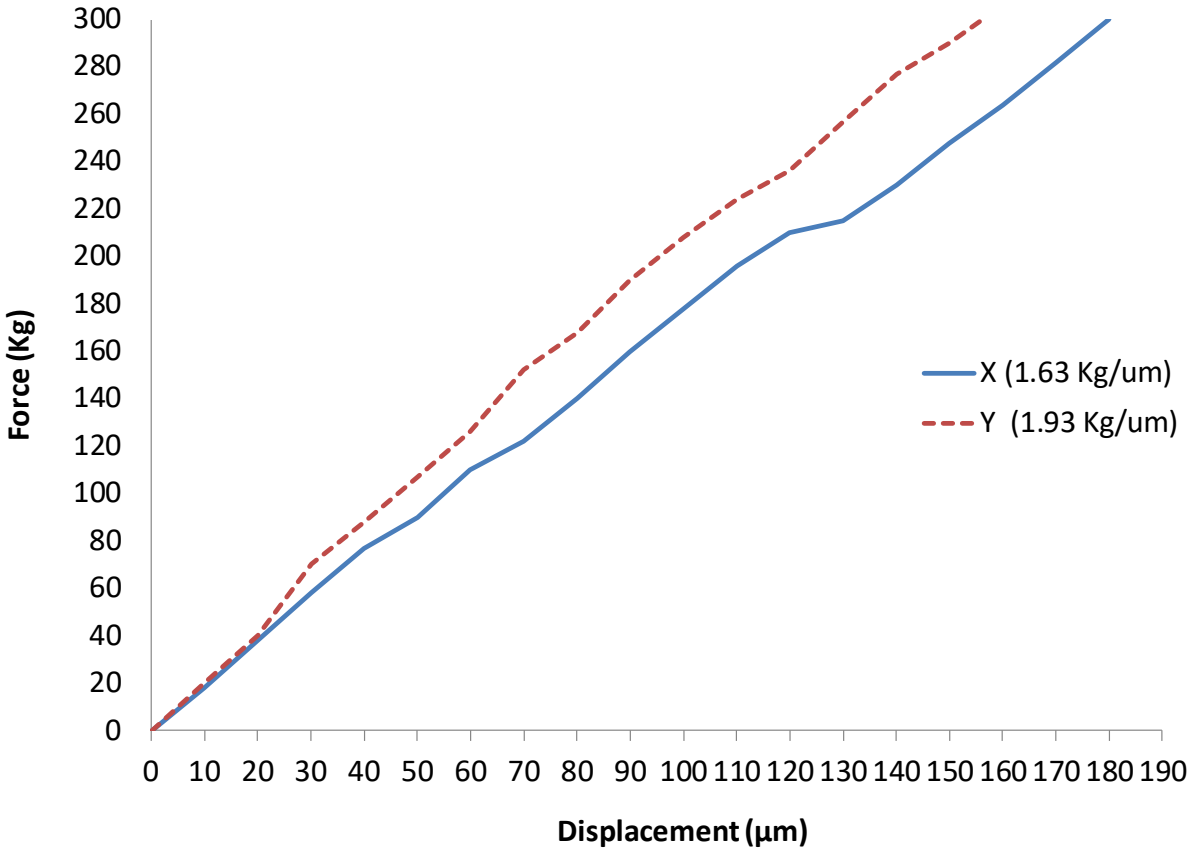

Fig. 4 Static rigidity data analysis

In comparing the analysis result with the actual test, the X-axis static stiffness error value was 0.7%, and the Y-axis static stiffness error value was 6.9%. The natural frequency analysis of the five-axis machine tool structure and the boundary conditions were set according to the actual fixed condition of the machine. We compared the main modes that have a greater impact on the processing performance, and we observed their mode shapes, including the torsion of the spindle and the column, as well as the torsion mode of the rotating table.

When performing modal experiments, it is necessary to devise a reasonable layout plan for the object to be tested while simultaneously confirming whether the position of the hitting point interferes with the position of the signal picked up by the accelerometer. The natural frequency of the structure is then analyzed and the analysis model is compared with the actual machine vibration mode. The data collected in the experiment are imported into MEscope

software, curve fitting is performed, and the sum of the imaginary part of the FRF is determined to calculate the frequency and damping value of each mode and to view the trend of each mode.

After comparing the finite element analysis (FEM) with the experimental mode (EMA), the maximum error ratio was 6.2%, the minimum error ratio was 2%, and the average error ratio was 4.7%. This finding verifies that the geometric model and the parameter settings, such as the material properties and boundary conditions, are aligned with the characteristics of the actual machine.

Table 1 Comparison of natural frequency between model and actual machine

Content	Modal analysis	Modal testing	Feature
Mode shape	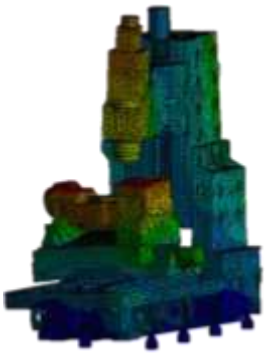		Spindle, column and rotary table swing horizontally back and forth
Frequency	69.1 Hz	67.7 Hz	2.1%
Mode shape	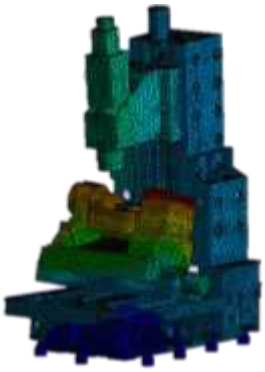		The main shaft and column swing up and down, and the rotary table swings back and forth
Frequency	72.1 Hz	76.9 Hz	6.2%

Mode shape	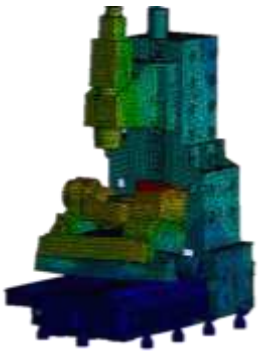		The main shaft and column swing up and down, and the rotary table swings back and forth
Frequency	90.0 Hz	85.1 Hz	5.8%

4 Cutting experiment

In the cutting experiment, we used ultra-fine tungsten steel and aluminum end mills; the cutting material was Al-6061, and the processing method was down-milling. The different axial and radial depths of the cut conditions were used to explore the surface roughness results.

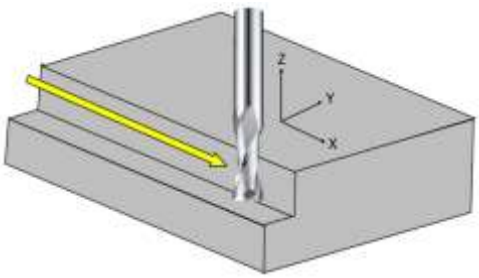

Number of blades	2
Helix angle (degrees)	40.0
Dc (mm)	6.0
Lc (mm)	16.0
L (mm)	50.0
d (mm)	6.0

Fig. 5 Cutting diagram and milling cutter specifications

Based on the modal analysis and experimental results, a cutting experiment was planned to assess the vibration shape trend of the entire machine, and the relative movement of the spindle end and the working platform was divided. First, the spindle speed was set to 4066 rpm (67.7 Hz) by down-milling. The main mode was the spindle vibration relative to the worktable. The surface roughness obtained by processing was Ra 0.54 μm, as shown in Fig. 6(b). The rotation speed was 5226 rpm (87.1 Hz) using the down-milling method. The main mode was the spindle vibrating up and down relative to the worktable. The surface roughness obtained by machining was Ra 16.96 μm. The surface after cutting using the tool is shown in Fig. 6(b).

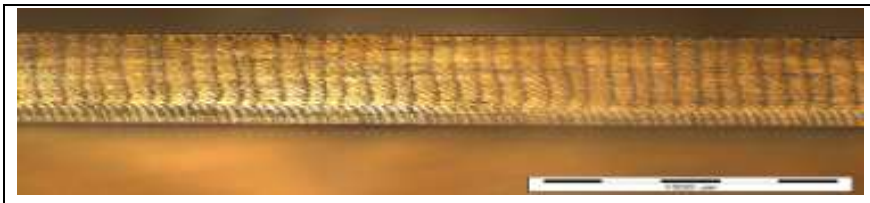

Ra 0.54 μm

(a)

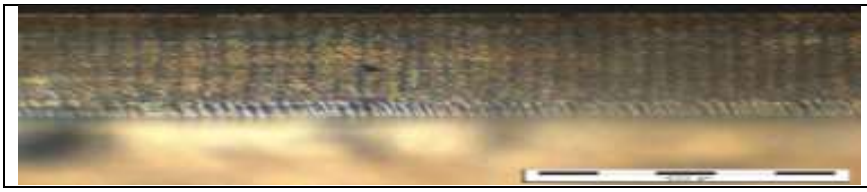

Ra 16.96 μm

(b)

Fig. 6 (a) Spindle speed: 4066 rpm (67.7 Hz). The spindle end moves left and right relative to the table; (b) Spindle speed: 5226 rpm (87.1 Hz). The spindle end moves up and down relative to the worktable

5 Prediction model and cutting testing

A polynomial network was employed to construct the predictive model, decompose the complex system into relatively simple subsystems through polynomial function nodes, and then combine the subsystems into many different levels. The input data were subdivided simultaneously and transmitted to each functional node. The function node used a polynomial function to calculate a limited amount of input data and obtain an output as the input of the next layer. Thus, the training structure of the entire polynomial network was established in sequence. Then, the optimal network construction, hierarchical features, and functional node were automatically generated according to the predicted square error rule.

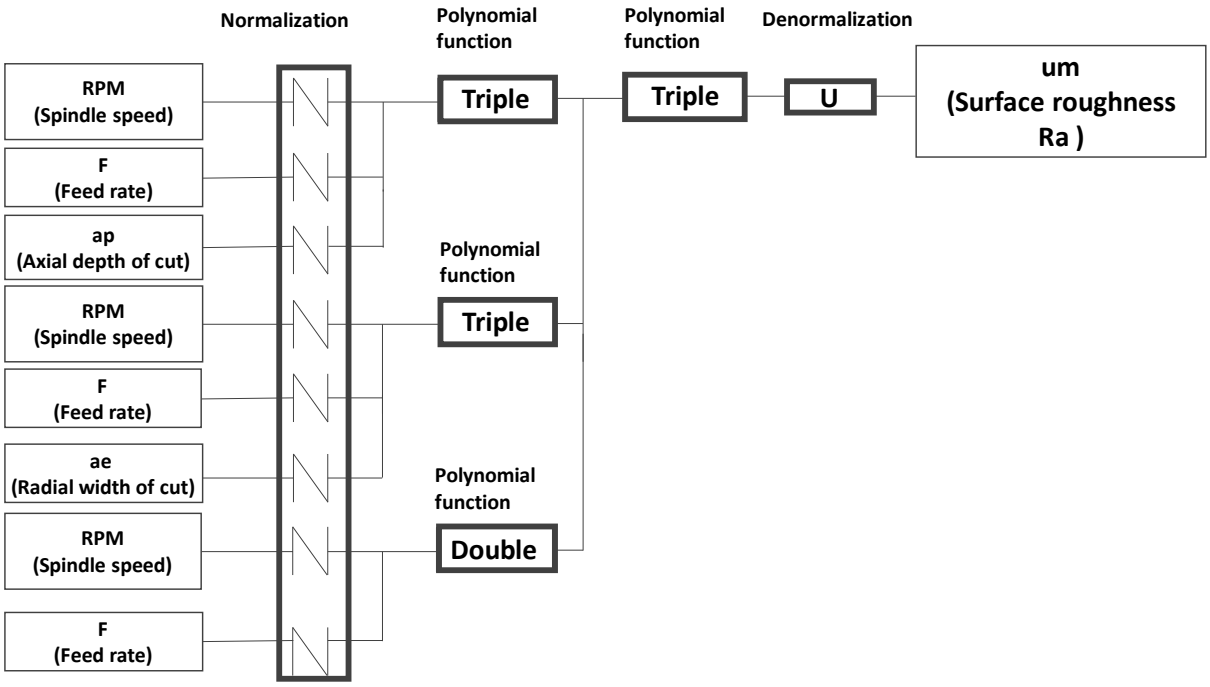

Fig. 7 Synthetic polynomial network planning diagram

Multi-function node type

The polynomial function reorganizes all polynomial node patterns as follows:

$$y_1 = w_0 + \sum_{i=1}^{m} W_i X_i + \sum_{i=1}^{m}\sum_{j=1}^{m} W_{ij} X_i X_j + \sum_{i=1}^{m}\sum_{j=1}^{m}\sum_{k=1}^{m} W_{ijk} X_i X_j X_k + \cdots\cdots$$

where X_i, X_j, X_k are the input values, y_1 is the output value, and W_i, W_j and W_k are the coefficients of the polynomial function node. Commonly used polynomial nodes are the normalizer, single node, double node, triple node, white node, and unitizer. The definitions are as follows:

1. Normalizer: Converts the original variable into a normalized input variable; the average is 0, the variance is 1, and its polynomial function is expressed as $y_1 = w_0 + w_i x_i$, where xi is the original input variable; y_1 is the normalized output variable; and w_0 and w_i are the coefficients.
2. Single node: Refers to a single input variable. The output and input variables have a third-order polynomial relationship. The polynomial function is expressed as $y_1 = w_0 + w_1 x_1 + w_2 {x_1}^2 + w_3 {x_1}^3$, where x_1 is an input variable, y_1 is an output variable, and

w_0,w_1,w_2, and w_3 are coefficients.

3. Double node: The two input variables, the output variable, and the input variable have a third-order polynomial relationship. The polynomial function is expressed as $y_1 = w_0 + w_1x_1 + w_2x_2 + w_3{x_1}^2 + w_4{x_2}^2 + w_5x_1x_2 + w_6{x_1}^3 + w_7{x_2}^3$, where x_1 , x_2 are input variables; y_1 is the output variable, and w_0,w_1,w_2,….w_7 are coefficients.
4. Triple node: Refers to the three input variables. The output variable and the input variable have a third-order polynomial relationship, and the polynomial function is expressed as $y_1 = w_0 + w_1x_1 + w_2x_2 + w_3x_3 + w_4{x_1}^2 + w_5{x_2}^2 + w_6{x_3}^2 + w_7x_1x_2 + w_8x_1x_3 + w_9x_2x_3 + w_{10}x_1x_2x_3 + w_{11}{x_1}^3 + w_{12}{x_2}^3 + w_{13}{x_3}^3$, where x_1, x_2, and x_3 are input variables, y_1 is the output variable, and w_0, w_1, w_2,……w_{13} are coefficients.
5. White node: Refers to *n* input variables, the output variable and the input variable are first-order polynomial relationships, and the polynomial function is expressed as $y_1 = w_0 + w_1x_1 + w_2x_2 + w_3x_3 + \cdots + w_nx_n$, where x_1, x_2,… x_n are input variables, y_1 is an output variable, and w_0,w_1,w_2,…w_n are coefficients.
6. Unitizer: Converts the output variable of the network into an actual output variable, and its polynomial function is expressed as $y_1 = w_0 + w_1x_1$, where x_1 is the input variable, y_1 is the output variable, and w_0 and w_1 are coefficients.

The polynomial function node is used to construct the prediction model of the processing parameters and surface roughness Ra values. The polynomial network filters variables that have no contribution. The output of any node can be used as the input of the next layer and is combined with the original input for subsequent comparison. The network is synthesized layer by layer until the network mode converges and satisfies the prediction square error (PSE) rule.

Before constructing a polynomial network, it is necessary to import training data, learn the synthesis algorithm through the polynomial network, and determine the best network structure according to the minimum prediction square error method. PSE is a heuristic measurement of

the expected square error of a network of independent data. PSE is defined as

$$\mathrm{PSE} = \mathrm{FSE} + \mathrm{KP} \tag{8}$$

The fitting square error (FSE) occurs when constructing a network model with the training data. FSE can be expressed as

$$\mathrm{FSE} = \frac{1}{\mathrm{n}} \sum_{i=1}^{N} (\overline{y_i} - y_i)^2 \tag{9}$$

where n is the number of training data, $\overline{y_i}$ is the expected value of the training combination, and y_i is the predicted value obtained from the network, Addionally, KP is the complexity penalty, and the KP value can be obtained from equation (8):

$$\mathrm{KP} = \mathrm{CPM} \times \frac{2K}{\mathrm{N}} \sigma p^2 \tag{10}$$

where K is the number of coefficients in the network, N is the number of training data, and σp^2 is the number of error variances between the prediction model and the actual model from the training database of the synthetic network. The complexity penalty factor (CPM) is an adjustable parameter that is used when synthesizing a polynomial network model. When N increases or σp^2 decreases, a polynomial network is used to construct the training data, which has higher credibility, and the network structure becomes more complex.

In equation (10), the matching accuracy increases as the PSE decreases. Under normal circumstances, the more complex the network model, the smaller the FSE value, and the higher the matching accuracy. In other words, the more complex the network is, the greater is the KP value. Therefore, PSE produces a trade-off between network model complexity and accuracy. In the network synthesis and calculation, the best network refers to the network with the smallest PSE value. Moreover, the CPM can be used to adjust the balance between the model complexity and accuracy. When the CPM value in the PSE increases, a more complex network is avoided. Conversely, when the CPM value decreases, a more complex network is adopted.

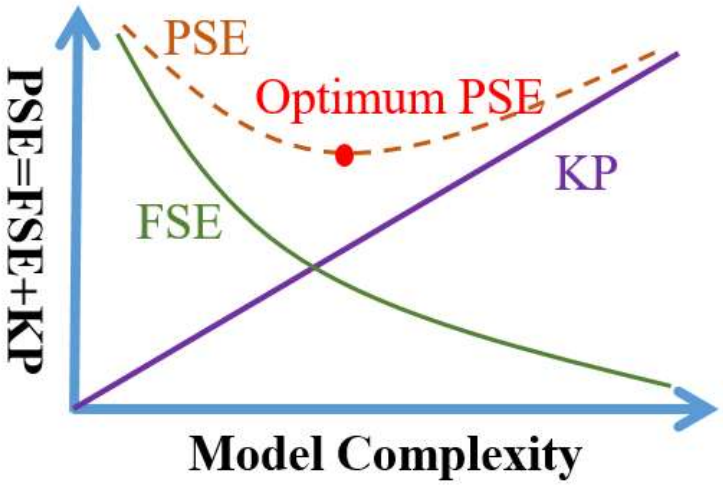

Fig. 8 Convergent prediction square error

In this study, the processing parameters of the UX300 machine were experimentally planned. The tool and cutting material were initially fixed, and then the processing parameters were used as the software input variables. The input data were as follows: rpm was the spindle speed, F was the feed rate, ap was the axial direction, and ae was the radial depth of cut. The measurement result of the SE-4000 non-contact surface roughness measuring instrument was set as the output data, which were the surface roughness Ra value of the workpiece. The input and output factors were placed into the polynomial network model for modeling. The reliability of the model was verified by predicting the parameters that had not been tested through the AIM polynomial network model. The results were then compared with those of the machine processing. The AIM software parameters were adjusted to a suitable fit and could then be converted into program codes and added to the machine controller.

Table 2 Cutting parameter plan

Material	Aluminum 6061-T6
Spindle speed	4000–9000 rpm
Feed per edge	0.0375/edge, 0.08 mm/edge
Feed rate	300–1440 m/min
Cut deep	1 mm, 2 mm, 3 mm
Cut width	0.5, 1.0 mm

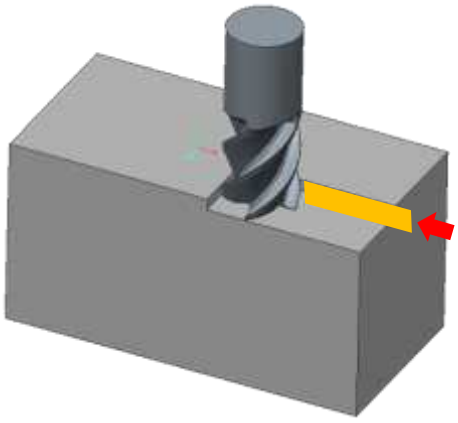

Measuring length range (section)	Cutoff x5
Measuring vertical range (magnification)	5000
Measurement level range (magnification)	50
Cutoff (mm)	0.8
Measuring speed (mm/s)	0.5

Fig. 9 Processing method and measurement parameters

Table 3 4000 rpm: Cutting training data

Spindle speed (rev/min)	Parameter		Cutting condition		Ra (μm)
	Feed rate (mm/min)	Feed per edge (mm)	ap (mm)	ae (mm)	
4000	300	0.0375	1	0.5	0.48
4000	300	0.0375	1	1	0.44
4000	300	0.0375	2	0.5	0.46
4000	300	0.0375	2	1	0.45
4000	300	0.0375	3	0.5	0.44
4000	300	0.0375	3	1	0.49
4000	640	0.08	1	0.5	0.57
4000	640	0.08	1	1	0.53
4000	640	0.08	2	0.5	0.44
4000	640	0.08	2	1	0.42
4000	640	0.08	3	0.5	0.40
4000	640	0.08	3	1	0.45

Table 4 5000 rpm: Cutting training data

Spindle speed (rev/min)	Parameter		Cutting condition		Ra (μm)
	Feed rate (mm/min)	Feed per edge (mm)	ap (mm)	ae (mm)	
5000	375	0.0375	1	0.5	0.39
5000	375	0.0375	1	1	0.52

5000	375	0.0375	2	0.5	0.41
5000	375	0.0375	2	1	0.47
5000	375	0.0375	3	0.5	0.32
5000	375	0.0375	3	1	0.38
5000	800	0.08	1	0.5	0.52
5000	800	0.08	1	1	0.64
5000	800	0.08	2	0.5	0.43
5000	800	0.08	2	1	0.55
5000	800	0.08	3	0.5	0.43
5000	800	0.08	3	1	0.41

Table 5 6000 rpm: Cutting training data

Spindle speed (rev/min)	Parameter		Cutting condition		Ra (μm)
	Feed rate (mm/min)	Feed per edge (mm)	ap (mm)	ae (mm)	
6000	450	0.0375	1	0.5	0.43
6000	450	0.0375	1	1	0.57
6000	450	0.0375	2	0.5	0.42
6000	450	0.0375	2	1	0.50
6000	450	0.0375	3	0.5	0.36
6000	450	0.0375	3	1	0.28
6000	960	0.08	1	0.5	0.61
6000	960	0.08	1	1	0.48
6000	960	0.08	2	0.5	0.45
6000	960	0.08	2	1	0.58
6000	960	0.08	3	0.5	0.36
6000	960	0.08	3	1	0.38

Table 6 7000 rpm: Cutting training data

Spindle speed (rev/min)	Parameter		Cutting condition		Ra (μm)
	Feed rate (mm/min)	Feed per edge (mm)	ap (mm)	ae (mm)	
7000	525	0.0375	1	0.5	0.35
7000	525	0.0375	1	1	0.37
7000	525	0.0375	2	0.5	0.32

7000	525	0.0375	2	1	0.47
7000	525	0.0375	3	0.5	0.33
7000	525	0.0375	3	1	0.30
7000	1120	0.08	1	0.5	0.42
7000	1120	0.08	1	1	0.55
7000	1120	0.08	2	0.5	0.37
7000	1120	0.08	2	1	0.55
7000	1120	0.08	3	0.5	0.33
7000	1120	0.08	3	1	0.37

Table 7 8000 rpm: Cutting training data

Spindle speed (rev/min)	Parameter		Cutting condition		Ra (μm)
	Feed rate (mm/min)	Feed per edge (mm)	ap (mm)	ae (mm)	
8000	600	0.0375	1	0.5	0.38
8000	600	0.0375	1	1	0.40
8000	600	0.0375	2	0.5	0.40
8000	600	0.0375	2	1	0.42
8000	600	0.0375	3	0.5	0.27
8000	600	0.0375	3	1	0.26
8000	1280	0.08	1	0.5	0.39
8000	1280	0.08	1	1	0.46
8000	1280	0.08	2	0.5	0.37
8000	1280	0.08	2	1	0.46
8000	1280	0.08	3	0.5	0.34
8000	1280	0.08	3	1	0.36

Table 8 9000 rpm: Cutting training data

Spindle speed (rev/min)	Parameter		Cutting condition		Ra (μm)
	Feed rate (mm/min)	Feed per edge (mm)	ap (mm)	ae (mm)	
9000	675	0.0375	1	0.5	0.48
9000	675	0.0375	1	1	0.39
9000	675	0.0375	2	0.5	0.35
9000	675	0.0375	2	1	0.32

9000	675	0.0375	3	0.5	0.33
9000	675	0.0375	3	1	0.25
9000	1440	0.08	1	0.5	0.50
9000	1440	0.08	1	1	0.44
9000	1440	0.08	2	0.5	0.45
9000	1440	0.08	2	1	0.47
9000	1440	0.08	3	0.5	0.37
9000	1440	0.08	3	1	0.35

The input enables an AIM polynomial network model to adjust the parameters so that the FSE and PSE in the network model fit and converge to find an optimized network model. The adjustment parameters include the complexity penalty factor (CPM), number of layers, overfit penalty factor (overfit penalty), limiting factor (carving limit), and other parameters. Fig. 10 shows the surface roughness polynomial model. The optimal model parameters were the complexity penalty factor (CPM) setting value of 0.01, number of layers, overfitting penalty factor of 1.0, and limit factor of 0.8. As shown in the figure 10, the nodes have several normalizers, triangles, a single double, and a single unitizer. The polynomial function nodes are as follows:

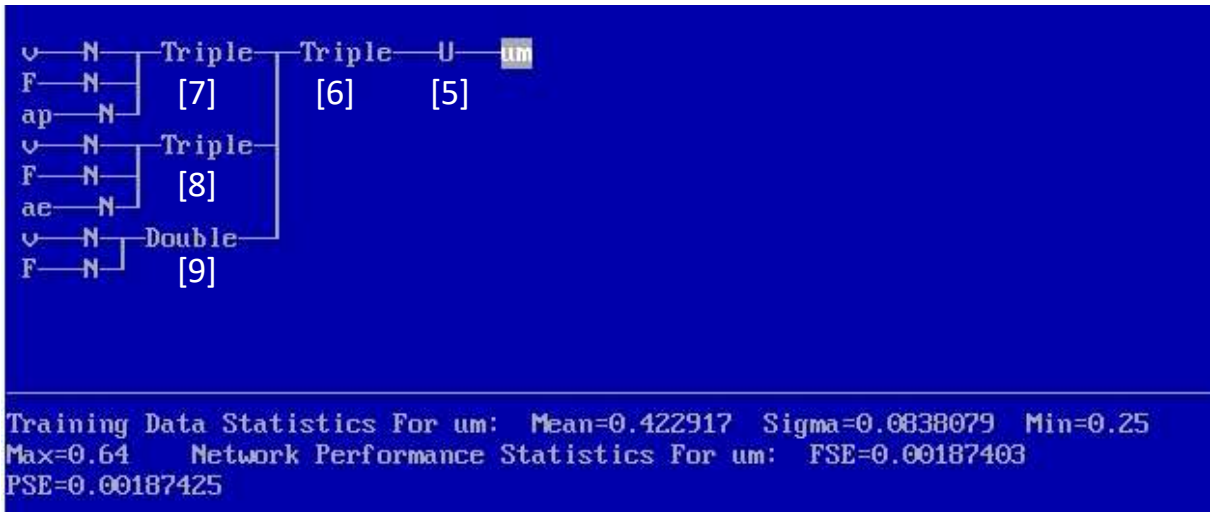

Fig. 10 AIM polynomial network

(1). Normalizer：

$$RPM = -3.78 + 0.000581 \times 1 \qquad F = -2.17 + 0.00284 \times 1$$

$$ap = -2.43 + 1.22 \times 1 \qquad ae = -2.98 + 3.97 \times 1$$

(2). Double node：

$$Double[9] = -0.0268 - 1.05 \times 1 + 0.468 \times 2 + 0.0491 \times 1^2 - 0.0044 * 2^2 + 0.258 * 1^3 - 0.031 \times 2^3$$

(3). Triple node :

$$Triple[6] = 0.0587 + 0.831 \times 1 + 1.79 \times 2 - 1.87 \times 3 - 0.151 \times 1^2 - 0.0823 \times 2^2 + 3.25 \times 3^2 + 0.83 \times 1 \times 2 - 0.308 \times 1 \times 3 - 3.76 \times 2 \times 3 - 0.858 \times 1 \times 2 \times 3 + 0.254 \times 1^3 + 0.865 \times 2^3 - 0.661 \times 3^3$$

$$Triple[7] = 0.162 - 1.05 \times 1 + 0.468 \times 2 - 0.431 \times 3 + 0.0491 \times 1^2 - 0.0044 \times 2^2 - 0.192 \times 3^2 + 0.0459 \times 1 \times 3 - 0.149 \times 2 \times 3 + 0.178 \times 1 \times 2 \times 3 + 0.258 \times 1^3 - 0.031 \times 2^3 - 0.15 \times 3^3$$

$$Triple[8] = -0.0268 - 1.05 \times 1 + 0.468 \times 2 - 0.119 \times 3 + 0.0491 \times 1^2 - 0.0044 \times 2^2 - 0.16 \times 1 \times 3 + 0.137 \times 2 \times 3 - 0.0731 \times 1 \times 2 \times 3 + 0.258 \times 1^3 - 0.031 \times 2^3 + 0.333 \times 3^3$$

(4). Unitizer：

$$u[5] = 0.423 + 0.0838 \times 1$$

6 Prediction model and verification

By importing into the AIM polynomial network model the machining parameter data that have not yet undergone cutting experiments, the predicted surface roughness Ra value can be obtained, and the actual machining and predicted results can be compared. The surface roughness error range is approximately within the Ra value of 0.1 μm. The experimental findings show that the parameter processing results are within the predictable range, that is, this polynomial network model has a certain degree of reference value, and the quality of the processed surface can be predicted from the polynomial model.

Table 9 Polynomial network model: Validation data

Spindle speed (rev/min)	Parameter		Cutting condition		Ra (μm)	AIM Predict Ra (μm)	Ra difference (μm)
	Feed rate (mm/min)	Feed per edge (mm)	ap (mm)	ae (mm)			
4000	320	0.04	1	0.75	0.45	0.45	0
4500	360	0.04	1	0.5	0.42	0.46	0.04
4500	360	0.04	0.5	1	0.45	0.52	0.07
5000	500	0.05	1	0.75	0.42	0.49	0.07
5000	500	0.05	1	0.5	0.40	0.48	0.08

5500	550	0.05	2	0.5	0.36	0.44	0.08
6000	720	0.06	2	0.75	0.36	0.45	0.09
6500	780	0.06	1.5	1	0.47	0.50	0.03
6500	780	0.06	2	0.5	0.40	0.40	0
7000	980	0.07	2	0.75	0.40	0.44	0.04
7500	1050	0.07	1.5	1	0.44	0.48	0.04
7500	1050	0.07	3	1	0.33	0.34	0.01
8000	1280	0.08	3	0.75	0.37	0.33	0.04
8500	1360	0.08	3	1	0.39	0.37	0.02
8500	1360	0.08	2.5	0.5	0.36	0.39	0.03
9000	1620	0.09	2	0.5	0.44	0.43	0.01
9500	1710	0.09	2.5	0.5	0.43	0.46	0.03
10000	2000	0.10	0.5	0.5	0.43	0.44	0.01

7 Conclusion

The starting point of this study was machine model analysis. A virtual machine model of the five-axis machine tool UX300 was constructed using ANSYS for static rigidity and dynamic analysis. The boundary conditions and material properties were improved by comparing the actual machine characteristics to simulate the real scenario. Static rigidity and modal experiments were performed to prove this finding of improvement. The static rigidity values of the two-axis of the five-axis machine tool spindle against the bed were X: 1.63 Kg/μm and Y: 1.93 Kg/μm; the maximum modal error ratio was 6.2%, the minimum error ratio was 2%, the average error ratio was 4.7%.

After studying and understanding the dynamic characteristics of the machine in depth, we planned the modal frequency band processing parameters and conducted modal cutting experiments to prove that the machine processing frequency had a substantial impact on the surface quality of the finished product. Subsequent planning of large data cutting experiments was used to develop intelligent processing by using the AIM polynomial neural network to train the surface roughness Ra value prediction model, constructing the correlation equation between cutting parameters, and determining the surface roughness model prediction results. The

prediction error was within a certain range of the surface roughness Ra value of 0.1 μm.

Authors' contributions: Formal analysis, writing, and funding acquisition, T.-C.C.; Data curation, and Software H.-H. L.; All authors have read and agreed to the published version of the manuscript.

Funding: The authors are greatly indebted to the Ministry of Science and Technology of the R.O.C. for supporting this research (Grant Nos. MOST 107-2218-E-150-005-MY3 and MOST 109-2622-E-150-014).

Conflicts of Interest: The authors declare no conflict of interest.

References

[1] M. Eynian, 2019, "In-process identification of modal parameters using dimensionless relationships in milling chatter," International Journal of Machine Tools and Manufacture, Volume 143, Pages 49-62

[2] X. Tang, F. Peng, R. Yan, Z. Zhu, Z. Li, S. Xin, 2021, "Nonlinear process damping identification using finite amplitude stability and the influence analysis on five-axis milling stability, " International Journal of Mechanical Sciences, Volume 190, 106008

[3] H. Liu, J. Wu, K. Liu, K. Kuang, Q. Luo, Z. Liu, Y. Wang, 2019, "Pretightening sequence planning of anchor bolts based on structure uniform deformation for large CNC machine tools," International Journal of Machine Tools and Manufacture, Volume 136, Pages 1-18

[4] P. Muñoz-Escalonaa, P.G. Maropoulosb, 2015, "A geometrical model for surface roughness prediction when face milling Al 7075-T7351 with square insert tools," Journal of Manufacturing Systems, Volume 36, Pages 216-223

[5] Z. Zhao, S. Wang, Z. Wang, N. Liu, S. Wang, C. Ma, B. Yang, 2020, "Interference- and chatter-free cutter posture optimization towards minimal surface roughness in five-axis machining," International Journal of Mechanical Sciences, Volume 171, 105395

[6] L. Wang, S. Ge, H. Si, X. Yuan, F.Duan, 2020, "Roughness control method for five-axis flank milling based on the analysis of surface topography," International Journal of Mechanical Sciences, Volume 169, 105337

[7] L. Wang, S. Ge, H. Si, L. Guan, F. Duan, Y. Liu, 2020, "Elliptical model for surface topography prediction in five-axis flank milling," Chinese Journal of Aeronautics, Volume 33, Issue 4, Pages 1361-1374

[8] M. Tomov, M. Kuzinovski, P. Cichosz, 2016, "Development of mathematical models for surface roughness parameter prediction in turning depending on the process condition," International Journal of Mechanical Sciences, Volume 113, Pages 120-132

[9] B. Das, S. Roy, R.N. Rai, S.C. Saha, 2016, "Study on machinability of in situ Al–4.5%Cu–TiC metal matrix composite-surface finish, cutting force prediction using ANN," CIRP Journal of Manufacturing Science and Technology, Volume 12, Pages 67-78

[10] E. García-Plaza, P.J. Núñez Lópeza, E.M. Beamud Gonzálezb, 2019, "Efficiency of vibration signal feature extraction for surface finish monitoring in CNC machining," Journal of Manufacturing Processes ,Volume 44, Pages 145–157

[11] P. Rasagopal, P. Senthilkumar, G. Nallakumarasamy, S. Magibalan, 2020, "A study surface integrity of aluminum hybrid composites during milling peration," Journal of Materials Research and Technology, Volume 9, Issue 3, Pages 4884-4893

[12] A. Mansour, H. Abdalla, 2002, "Surface roughness model for end milling: A semi-free cutting carbon casehardening steel (EN32) in dry condition," Journal of Materials Processing Technology, Volume 124, Pages 183-191

[13] O.B. Abouelatta, J. Mádl, 2001, "Surface roughness prediction based on cutting parameters and tool vibrations in turning operations, "Journal of Materials Processing Technology, Volume 118, Issues 1-3, Pages 269-277

[14] W.S. Lin, B.Y. Lee, C.L. Wu, 2001, "Modeling the surface roughness and cutting force for turning," Journal of Materials Processing Technology, Volume 108, Pages 286-293

[15] V. Ostasevicius, R. Gaidys, J. Rimkeviciene, R. Dauksevicius, 2010, "An approach based on tool mode control for surface roughness reduction in high-frequency vibration cutting," Journal of Sound and Vibration, Volume 329, Pages 4866-4879

[16] Y. Sahin, A.R. Motorcu, 2008, "Surface roughness model in machining hardened steel with cubic boron nitride cutting tool," International Journal of Refractory Metals & Hard Materials, Volume 26, Pages 84-90

[17] H.O. Ktem, T. Erzurumlu, H. Kurtaran, 2005, "Application of response surface methodology in the optimization of cutting conditions for surface roughness," Journal of Materials Processing Technology , Volume 170, Pages 11-16

[18] D.I. Lalwani, N.K. Mehta, P.K. Jain, 2008, "Experimental investigations of cutting parameters influence on cutting forces and surface roughness in finish hard turning of MDN250 steel," Journal of Materials Processing Technology, Volume 206, Pages 167-179

[19] J. Paulo Davim, V.N. Gaitonde, S.R. Karnikc, 2008, "Investigations into the effect of cutting conditions on surface roughness in turning of free machining steel by ANN models," Journal of Materials Processing Technology, Volume 205, Pages 16-23

[20] N. Liu, S.B. Wang, Y.F. Zhang, W.F. Lu, 2016, "A novel approach to predicting surface roughness based on specific cutting energy consumption when slot milling Al-7075," International Journal of Mechanical Sciences, Volume 118, Pages 13-20

[21] A.E Diniz, R. Micaroni, 2002, "Cutting conditions for finish turning process aiming: The use of dry," International Journal of Machine Tools & Manufacture, Volume 42, 899904

[22] N. Muthukrishnan, J.P. Davim, 2009, "Optimization of machining parameters of Al/SiC-MMC with ANOVA and ANN analysis," Journal of Materials Processing Technology, Volume 209, Pages 225-232

[23] S. Rawangwong, J. Chatthong, W. Boonchouytan, R. Burapa, 2014, "Influence of cutting parameters in face milling semi-solid AA7075 using carbide tool affected the surface roughness and tool wear," Energy Procedia, Volume 56, Pages 448-457

[24] Y. C. Wang, C. H. Chen, B. Y. Lee, 2009, "The predictive model of surface roughness and searching system in database for cutting tool grinding," Materials Science Forum, Volume 626-627, Pages 11-16

[25] J.-Y. Chen, T.-C. Chan, B.-Y. Lee, C.-Y. Liang, 2020, "Prediction model of cutting edge for end mills based on mechanical material properties," International Journal of Advanced Manufacturing Technology, Volume 107, Pages 2939–2951